large ξ they diverged at small ξ. Hence empirical curves were drawn through the observed points, and from the curves for layers 5 and 6 those for the other layers were deduced. The corrected intensities for elongated and contracted reflections were scaled independently, layer by layer, to the calculated structure factors. When the same reflection occurred in both sets, agreement was good, and mean values were finally used.

References

ALBRECHT, G. (1939). *Rev. Sci. Instrum.* **10**, 221.

BERGHUIS, J., HAANAPPEL, IJ. M., POTTERS, M., LOOPSTRA, B. O., MACGILLAVRY, C. H. & VEENENDAAL, A. L. (1955). *Acta Cryst.* **8**, 478.

BRAGG, W. L. & WEST, J. (1930). *Phil. Mag.* **10**, 823.

BUERGER, M. J. (1956). *Proc. Nat. Acad. Sci. Wash.* **42**, 776.

COLE, W. F., SØRUM, H. & TAYLOR, W. H. (1951). *Acta Cryst.* **4**, 20.

FORSYTH, J. B. & WELLS, M. (1959). *Acta Cryst.* **12**, 412.

GAY, P. (1953). *Miner. Mag.* **30**, 169.

JELLINEK, F. (1958). *Acta Cryst.* **11**, 677.

LIPSON, H. & COCHRAN, W. (1953). *The Determination of Crystal Structures.* London: Bell.

MEGAW, H. D. (1956). *Acta Cryst.* **9**, 56.

MEGAW, H. D., KEMPSTER, C. J. E. & RADOSLOVICH, E. W. (1962). *Acta Cryst.* **15**, 1017.

NEWNHAM, R. E. & MEGAW, H. D. (1960). *Acta Cryst.* **13**, 303.

PHILLIPS, D. C. (1954). *Acta Cryst.* **7**, 746.

RADOSLOVICH, E. W. (1955). Thesis, Cambridge University.

RAMACHANDRAN, G. N. & SRINIVASAN, R. (1959). *Acta Cryst.* **12**, 410.

SØRUM, H. (1951). *K. Norske Vidensk. Selsk. Skr.* No. 3. Thesis, Trondheim.

SØRUM, H. (1953). *Acta Cryst.* **6**, 413.

TAYLOR, W. H. (1933). *Z. Kristallogr.* **85**, 425.

TAYLOR, W. H., DARBYSHIRE, J. A. & STRUNZ, H. (1934). *Z. Kristallogr.* **87**, 464.

WELLS, M. (1961). Thesis, Cambridge University.

WILSON, A. J. C. (1949). *Acta Cryst.* **2**, 318.

Acta Cryst. (1962). **15**, 1017

The Structure of Anorthite, $CaAl_2Si_2O_8$. II. Description and Discussion

BY HELEN D. MEGAW, C. J. E. KEMPSTER* AND E. W. RADOSLOVICH†

Crystallographic Laboratory, Cavendish Laboratory, Cambridge, England

(*Received* 5 *October* 1961 *and in revised form* 21 *November* 1961)

Anorthite has a felspar structure with the following particular features: (1) Si and Al tetrahedra alternate, so that each O atom has one Si and one Al neighbour; there is no Si/Al disorder. (2) Si–O and Al–O bond lengths show real variations within the same tetrahedron, the average value of each increasing as the number of Ca neighbours of the O atom increases from zero to 2. (3) There are 4 independent Ca atoms, 6- or 7-coordinated: pairs related (topologically, not exactly) by the *C*-face-centring translation have very similar environments, while those related by body-centring or by *z*-axis halving are very markedly different. There is no disorder of Ca position. (4) If the tetrahedra are grouped into the two topologically different types (distinguished conventionally by the subscripts 1 and 2 for their tetrahedral atoms) all tetrahedra of the same type have qualitatively similar bond-angle strains (i.e. departures from the tetrahedral angle of 109° 28′), independent of their Si/Al content. Comparison with other felspars shows that the strains are characteristic of the felspar structure, but are nearly twice as great in the felspars with divalent cations as in those with monovalent cations. (5) Most of the bond angles at O are in the range 125–145°, but there are some exceptionally large angles of about 165–170°.

These facts are explained by a model in which the building elements are nearest-neighbour bonds and bond angles, endowed with elastic moduli, acted on by the only unshielded cation–cation electrostatic repulsion, namely that acting across the centre of symmetry. The bond-angle strains at Si and Al are qualitatively predicted by it, and agree with observation. Most of the distortions of the felspar structure are common (qualitatively) to all felspars, depending on cation charge; others depend on cation size. In contrast to these, the effects of Si/Al distribution are relatively so small that discussion of them cannot usefully begin until the other larger effects have been clarified.

1. Introduction

Anorthite, $CaAl_2Si_2O_8$, is an important member of the felspar family. Other members of the family, whose structures have been determined in detail, and to which reference will be made here, are listed in Table 1. It was hoped that detailed comparison of the differences between members of the family would help our understanding not only of the felspars as a whole but also of the general character of three-dimensionally-linked framework structures. This has proved to be the case, as will be shown in what follows.

The method by which the structure was determined was described in Paper I (Kempster, Megaw &

* Present address: Department of Physics, University of Adelaide, Adelaide, Australia.

† Present address: Division of Soils, Commonwealth Scientific and Industrial Research Organisation, Adelaide, Australia.

Table 1

Composition	Name	Source	Reference
$KAlSi_3O_8$	Sanidine	Mogok, Burma (Spencer C), heat-treated	Cole, Sørum & Kennard (1949)
	Orthoclase	Mogok, Burma (Spencer C)	Jones & Taylor (1961)
	Microcline (intermediate)*	Kodarma, India (Spencer U)	Bailey & Taylor (1955)
$NaAlSi_3O_8$	Low albite	Ramona, California (Emmons 29)	Ferguson, Traill & Taylor (1958)
	Quenched high albite	Amelia Co., Virginia (Emmons 31) heat-treated	Ferguson, Traill & Taylor (1958)
$CaAl_2Si_2O_8$	Anorthite ('low anorthite', 'primitive anorthite')	Monte Somma, Italy (B.M. 30744)	Kempster (1957) and this paper
$BaAl_2Si_2O_8$	Celsian	Broken Hill, New South Wales (Segnit, 1946)	Newnham & Megaw (1960)

* A preliminary report on the structure of maximum microcline by B. E. Brown and S. W. Bailey appeared in the program of a joint meeting of the Geological and Mineralogical Societies of America in November 1961. All references in the present paper are to intermediate microcline.

Radoslovich, 1962), which includes a table of atomic coordinates and their standard deviations. No attempt was made, during that analysis, to distinguish between Si and Al atoms, which were both given the symbol T ('tetrahedral atom').

The space group is $P\bar{1}$; the unit cell is primitive,

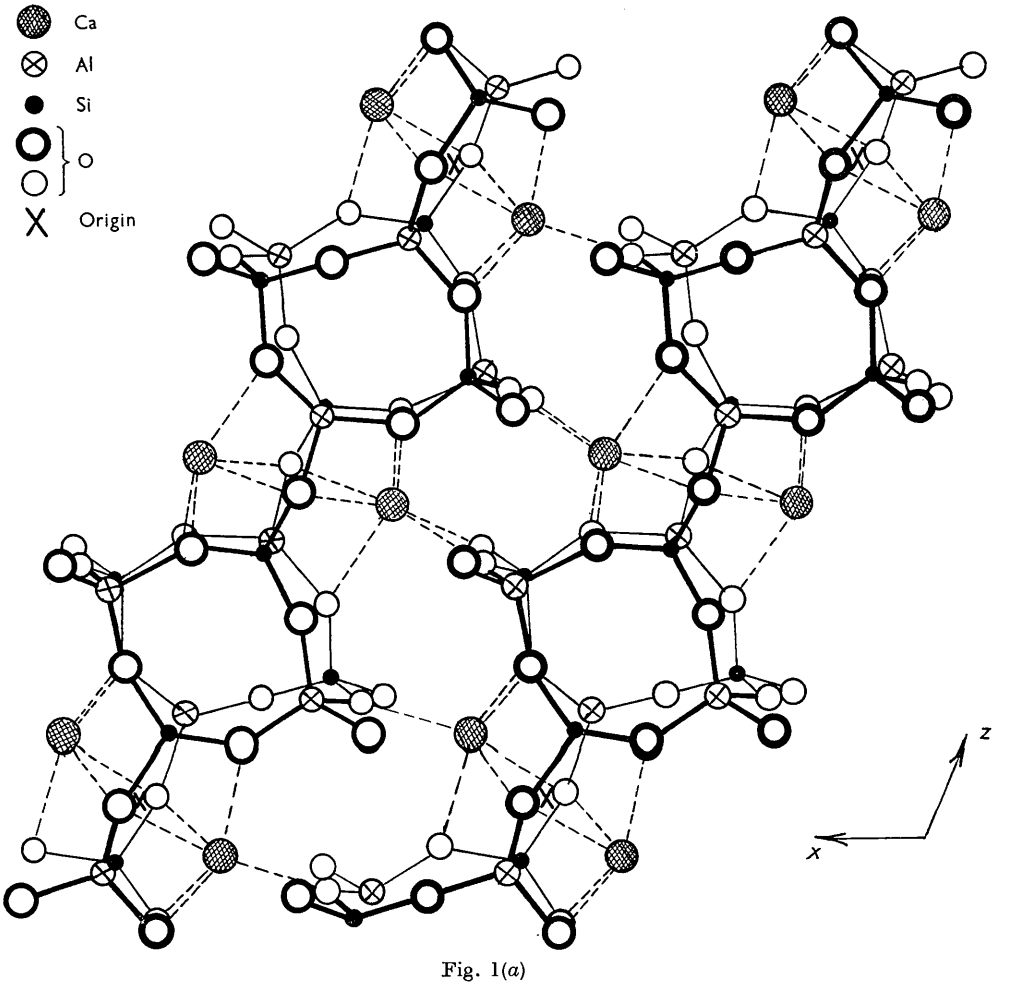

Fig. 1(*a*)

Fig. 1. Projection down [010] of parts of structure bounded roughly by the following planes: (*a*) $y=\pm 0{\cdot}3$; (*b*) $y=0{\cdot}2, 0{\cdot}8$; (*c*) $y=0{\cdot}1, 0{\cdot}4$. Heavy lines indicate upper part of layer shown. The projection of the corners of the unit cell (origin of coordinates) are marked with crosses in all diagrams. (*Note.* This is an *inclined* projection down [010] on (010). The drawing differs very little from an *orthogonal* projection on the plane normal to [010], but in the latter case the axes x and z would stick slightly out of the paper.)

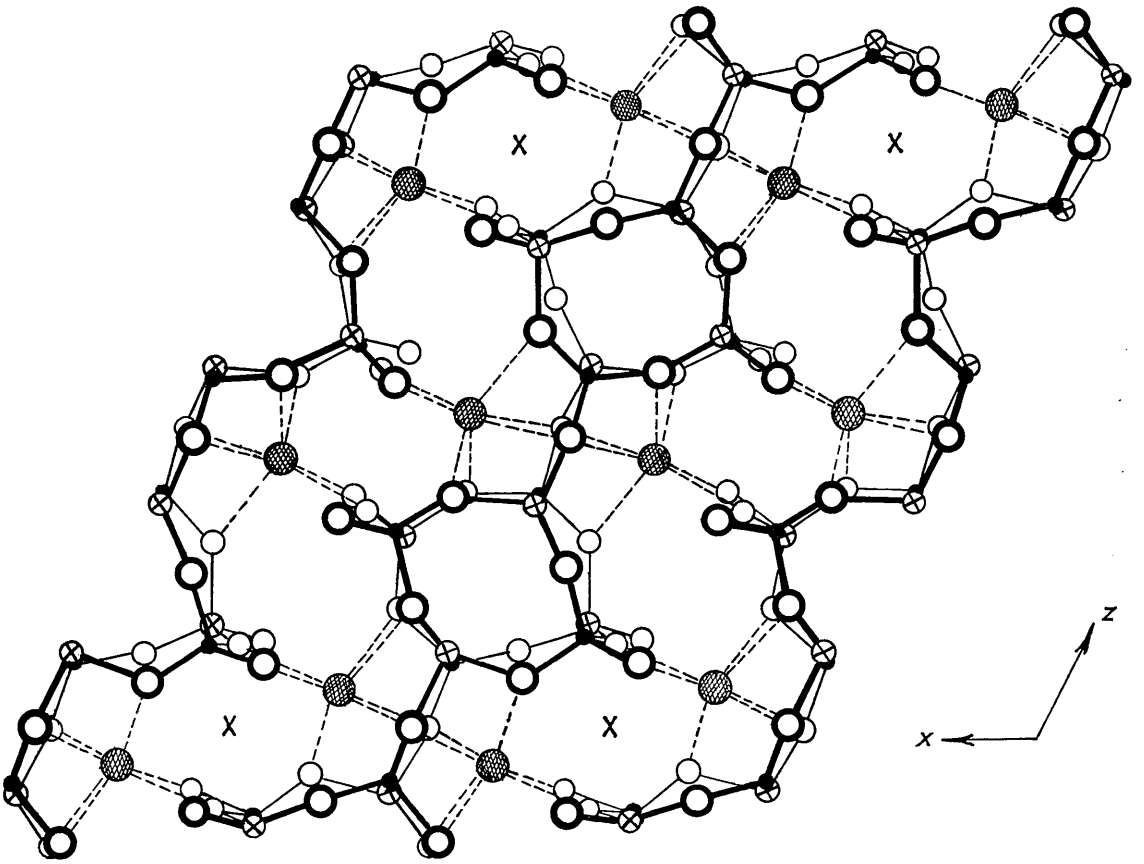
X
X
X
X
z
x

Fig. 1(*b*)

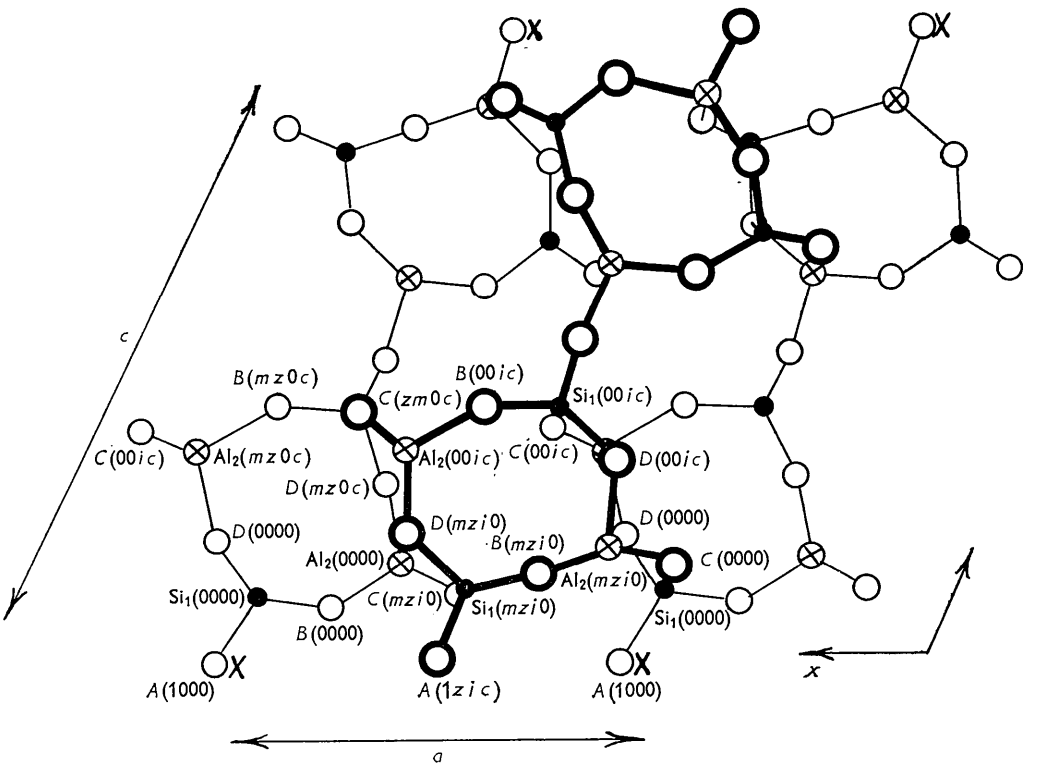
X
X
c
B(mz0c)
B(00ic)
C(zm0c)
Si1(00ic)
C(00ic)
Al2(mz0c)
Al2(00ic)
C(00ic)
D(00ic)
D(mz0c)
D(mzi0)
D(0000)
B(mzi0)
D(0000)
Al2(0000)
Al2(mzi0)
C(0000)
Si1(0000)
C(mzi0)
Si1(mzi0)
Si1(0000)
B(0000)
X
X
A(1000)
A(1zic)
A(1000)
x
a

Fig. 1(*c*)

with dimensions approximately $8 \times 13 \times 14$ Å, which means that the volume per lattice point is four times that of typical felspars such as albite. Thus the true cell consists of four subcells, equal in volume and with closely similar but not identical contents. Each subcell contains two formula units (CaT_4O_8) related by a centre of symmetry; but, relative to an origin at the corner of the subcell, corresponding atoms in the four subcells have slightly different coordinates.

It can be seen that atomic positions in subcells related by the base-centring vector (zi) are more closely similar than those related by the body-centring vector ($0i$) or the c-axis halving ($z0$).

Bond lengths and bond angles are given in Table 2,

Table 2. *Bond lengths and angles*

(*a*) Ca–O bonds in Å

Ca(000)		Ca($zi0$)		Ca($z0c$)		Ca($0ic$)	
$O_A(1000)$	2·618	$O_A(1zi0)$	2·471	$O_A(1z0c)$	2·476	$O_A(10ic)$	2·459
$O_A(100c)$	2·500	$O_A(1zic)$	2·586	$O_A(1z00)$	2·720	$O_A(10i0)$	2·822
$O_A(2000)$	2·279	$O_A(2zi0)$	2·322	$O_A(2z0c)$	2·350	$O_A(20ic)$	2·335
$O_A(2z0c)$	3·491	$O_A(20ic)$	3·762	$O_A(2000)$	> 4	$O_A(2zi0)$	> 4
$O_A(200c)$	> 4	$O_A(2zic)$	3·746	$O_A(2z00)$	3·375	$O_A(20i0)$	3·237
$O_B(0000)$	3·995		> 4		> 4		> 4
$O_B(000c)$	2·368	$O_B(0zic)$	2·421	$O_B(0z00)$	2·464	$O_B(00i0)$	2·413
$O_B(m00c)$	3·836	$O_B(mzic)$	3·247	$O_B(mz00)$	2·491	$O_B(m0i0)$	2·496
$O_C(0zi0)$	3·088	$O_C(0000)$	3·543	$O_C(00ic)$	3·824	$O_C(0z0c)$	3·798
$O_C(mzi0)$	3·279	$O_C(m000)$	2·807	$O_C(m0ic)$	2·565	$O_C(mz0c)$	2·568
$O_D(0000)$	2·423	$O_D(0zi0)$	2·391	$O_D(0z0c)$	2·397	$O_D(00ic)$	2·382
$O_D(m000)$	2·532	$O_D(mzi0)$	2·771	$O_D(mz0c)$	3·725	$O_D(m0ic)$	3·876
Mean	2·544	Mean	2·538	Mean	2·495	Mean	2·496

(*b*) Individual *T*–O bonds, in Å

Key no. of tetrahedron	Atoms *T*	Atoms O	Length	Key no. of tetrahedron	Atoms *T*	Atoms O	Length
1.	$T_1(0000)$	$O_A(1000)$	1·647	9.	$T_1(0z00)$	$O_A(1z00)$	1·820
		$O_B(0000)$	1·641			$O_B(0z00)$	1·755
		$O_C(0000)$	1·575			$O_C(0z00)$	1·701
		$O_D(0000)$	1·589			$O_D(0z00)$	1·755
2.	$T_1(00i0)$	$O_A(10i0)$	1·620	10.	$T_1(0zi0)$	$O_A(1zi0)$	1·747
		$O_B(00i0)$	1·599			$O_B(0zi0)$	1·733
		$O_C(00i0)$	1·585			$O_C(0zi0)$	1·708
		$O_D(00i0)$	1·661			$O_D(0zi0)$	1·796
3.	$T_1(mz0c)$	$O_A(1z00)$	1·618	11.	$T_1(m00c)$	$O_A(1000)$	1·794
		$O_B(mz0c)$	1·626			$O_B(m00c)$	1·723
		$O_C(mz0c)$	1·617			$O_C(m00c)$	1·735
		$O_D(mz0c)$	1·571			$O_D(m00c)$	1·754
4.	$T_1(mzic)$	$O_A(1zi0)$	1·643	12.	$T_1(m0ic)$	$O_A(10i0)$	1·757
		$O_B(mzic)$	1·600			$O_B(m0ic)$	1·757
		$O_C(mzic)$	1·623			$O_C(m0ic)$	1·755
		$O_D(mzic)$	1·637			$O_D(m0ic)$	1·695
5.	$T_2(0z00)$	$O_A(2z00)$	1·624	13.	$T_2(0000)$	$O_A(2000)$	1·784
		$O_B(0z00)$	1·589			$O_B(0000)$	1·749
		$O_C(m0i0)$	1·629			$O_C(mzi0)$	1·723
		$O_D(m00c)$	1·611			$O_D(mz0c)$	1·730
6.	$T_2(0zi0)$	$O_A(2zi0)$	1·606	14.	$T_2(00i0)$	$O_A(20i0)$	1·782
		$O_B(0zi0)$	1·652			$O_B(00i0)$	1·792
		$O_C(m000)$	1·617			$O_C(mz00)$	1·745
		$O_D(m0ic)$	1·566			$O_D(mzic)$	1·692
7.	$T_2(m00c)$	$O_A(200c)$	1·646	15.	$T_2(mz0c)$	$O_A(2z0c)$	1·754
		$O_B(m00c)$	1·559			$O_B(mz0c)$	1·747
		$O_C(0zic)$	1·601			$O_C(00ic)$	1·706
		$O_D(0z00)$	1·603			$O_D(0000)$	1·769
8.	$T_2(m0ic)$	$O_A(20ic)$	1·634	16.	$T_2(mzic)$	$O_A(2zic)$	1·738
		$O_B(m0ic)$	1·628			$O_B(mzic)$	1·696
		$O_C(0z0c)$	1·622			$O_C(000c)$	1·780
		$O_D(0zi0)$	1·629			$O_D(00i0)$	1·792

Table 2 (*cont.*)

(*c*) T–O bonds, tetrahedral means and r.m.s. deviations, in Å

Key no.	Atom	r_t	$\varepsilon(r)$	$\lvert r_t$-group mean$\rvert$	Key no.	Atom	r_t	$\varepsilon(r)$	$\lvert r_t$-group mean$\rvert$
1.	$T_1(0000)$	1·613	0·031	0·001	9.	$T_1(0z00)$	1·758	0·034	0·009
2.	$T_1(00i0)$	1·616	0·029	0·002	10.	$T_1(0zi0)$	1·746	0·032	0·003
3.	$T_1(mz0c)$	1·608	0·022	0·006	11.	$T_1(m00c)$	1·752	0·027	0·003
4.	$T_1(mzic)$	1·626	0·017	0·012	12.	$T_1(m0ic)$	1·741	0·027	0·008
5.	$T_2(0z00)$	1·613	0·015	0·001	13.	$T_2(0000)$	1·746	0·024	0·003
6.	$T_2(0zi0)$	1·610	0·031	0·004	14.	$T_2(00i0)$	1·753	0·039	0·004
7.	$T_2(m00c)$	1·602	0·031	0·012	15.	$T_2(mz0c)$	1·744	0·023	0·005
8.	$T_2(m0ic)$	1·628	0·004	0·014	16.	$T_2(mzic)$	1·752	0·038	0·003
	Mean	1·614				Mean	1·749		
	R.m.s. value		0·024	0·008		R.m.s. value		0·031	0·005

(*d*) O–O distances in tetrahedron edges, in Å

Key no. of tetrahedron	O_A–O_B	O_A–O_C	O_A–O_D	O_B–O_C	O_B–O_D	O_C–O_D
1.	2·537	2·770	2·525	2·631	2·721	2·593
2.	2·518	2·702	2·540	2·651	2·680	2·711
3.	2·486	2·744	2·556	2·666	2·713	2·577
4.	2·598	2·709	2·564	2·696	2·678	2·669
5.	2·586	2·519	2·655	2·644	2·659	2·723
6.	2·636	2·520	2·639	2·743	2·550	2·678
7.	2·700	2·549	2·660	2·603	2·535	2·648
8.	2·618	2·613	2·651	2·706	2·663	2·697
9.	2·725	3·020	2·724	2·842	3·016	2·842
10.	2·594	3·013	2·638	2·893	2·962	2·914
11.	2·839	2·946	2·705	2·867	2·892	2·886
12.	2·679	2·914	2·819	2·935	2·871	2·818
13.	2·895	2·752	2·803	2·886	2·862	2·897
14.	2·712	2·690	2·831	2·962	2·936	2·944
15.	2·857	2·759	2·753	2·819	2·903	2·974
16.	2·791	2·797	2·840	2·876	2·870	2·980

(*e*) Other short O–O distances and Ca–Ca distances, in Å

Atoms	Length	Comment
$O_B(0z00)$–$O_B(mz00)$	3·200	Ca($z0c$) polyhedron edge
$O_B(00i0)$–$O_B(m0i0)$	3·063	Ca($0ic$) polyhedron edge
$O_B(mz00)$–$O_C(m0ic)$	3·003	Ca($z0c$) polyhedron edge
$O_B(m0i0)$–$O_C(mz0c)$	2·983	Ca($0ic$) polyhedron edge
$O_C(0zi0)$–$O_D(m000)$	3·146	Ca(000) polyhedron edge
$O_D(0000)$–$O_D(m000)$	3·054	Ca(000) polyhedron edge
$O_D(0zi0)$–$O_D(mzi0)$	2·993	Ca($zi0$) polyhedron edge
$O_A(1000)$–$O_A(100c)$	3·217	Shared edges across centres of symmetry
$O_A(1zi0)$–$O_A(1zic)$	3·245	
$O_A(1z00)$–$O_A(1z0c)$	3·260	
$O_A(10i0)$–$O_A(10ic)$	3·278	
Ca(000)–Ca($00c$)	3·983	Short cation–cation distances across centres of symmetry
Ca($zi0$)–Ca(zic)	3·880	
Ca($z00$)–Ca($z0c$)	4·055	
Ca($0i0$)–Ca($0ic$)	4·160	

using the notation of Megaw (1956). Their standard deviations, calculated from the standard deviations of the coordinates, $\sigma(x_n)$ (see Paper I, § 6), are as follows: Ca–O, 0·0039; T–O, 0·0041; O–O, 0·0053 Å; angle at T, 0·4°; angle at O, 0·6°. Projections of the structure are shown in Fig. 1.

Preliminary results, and conclusions about the Si/Al arrangement, have already been reported (Kempster, Megaw & Radoslovich, 1960).

2. Description of structure

2·1. T–O *bond lengths, and* Al/Si *distribution*

It was mentioned in Paper I that the T–O tetrahedra divided themselves into two groups, the difference between which became more marked as refinement progressed. It is obvious from inspection of Table 2(*b*) (and is confirmed below) that the difference is significant, and therefore the small and large tetrahedra

Table 2 (*cont.*)

(*f*) Bond angles at *T*, in degrees

Key no. of tetrahedron	Atom	Edge subtending angle at *T*					
		O_A–O_B	O_A–O_C	O_A–O_D	O_B–O_C	O_B–O_D	O_C–O_D
1.	$T_1(000)$	101·0	118·6	102·6	109·8	114·7	110·1
2.	$T_1(00i)$	102·9	115·0	101·4	112·7	110·6	113·3
3.	$T_1(mz0)$	100·0	116·0	106·5	110·5	116·1	107·9
4.	$T_1(mzi)$	106·4	112·1	102·8	113·5	111·7	109·8
5.	$T_2(0z0)$	107·2	101·5	110·3	110·5	112·4	114·3
6.	$T_2(0zi)$	108·0	102·9	112·6	114·1	104·8	114·6
7.	$T_2(m00)$	114·8	103·4	109·9	110·8	106·6	111·4
8.	$T_2(m0i)$	106·8	106·7	108·7	112·8	109·7	112·1
9.	$T_1(0z0)$	99·3	118·1	99·2	110·7	118·5	110·7
10.	$T_1(0zi)$	96·4	121·3	96·3	114·4	114·1	112·4
11.	$T_1(m00)$	107·6	113·2	99·3	112·0	112·5	111·6
12.	$T_1(m0i)$	99·3	112·2	109·5	113·4	112·6	109·6
13.	$T_2(000)$	110·0	103·3	105·8	112·5	110·7	114·1
14.	$T_2(00i)$	98·7	99·4	109·1	113·8	114·8	117·8
15.	$T_2(mz0)$	109·4	105·7	102·7	109·4	111·3	117·7
16.	$T_2(mzi)$	108·7	105·3	107·1	111·6	110·7	113·2

(*g*) Bond angles at O, in degrees

	O_A		O_B	O_C	O_D
1000	136·2	0000	129·4	132·8	137·8
10*i*0	140·0	00*i*0	135·9	130·8	124·6
1*z*00	135·3	0*z*00	139·6	131·2	125·2
1*zi*0	136·1	0*zi*0	128·3	130·8	132·6
2000	125·3	*m*000	170·8	130·5	140·3
20*i*0	122·5	*m*0*i*0	145·3	130·9	166·9
2*z*00	124·0	*mz*00	143·5	127·5	161·4
2*zi*0	125·9	*mzi*0	163·6	130·5	138·5

must be identified as Si-rich and Al-rich respectively. Small and large tetrahedra alternate in every direction, so that each O atom is shared by one small and one large one. Since no assumptions about the nature of the *T* atom were made at any stage in deriving this result, it constitutes a direct proof of the 'aluminium avoidance rule' put forward earlier (Loewenstein, 1954; Goldsmith & Laves, 1955).

The significance of bond-length differences can be examined by Cruickshank's (1949) test, based on the ratio $\delta l/\sigma$, where δl is the difference of the two quantities to be compared, σ_1 and σ_2 are their standard deviations, and $\sigma^2=\sigma_1^2+\sigma_2^2$. The mean bond lengths and deviations from the mean are recorded in Table 2(*c*).

We first notice that $\varepsilon(r)$, the r.m.s. deviation of a bond from the tetrahedral mean, is much greater than $\sigma(r)$, the standard deviation derived from $\sigma(x_n)$. The significance of this is demonstrated in Table 3 (1). It shows that the differences of bond length within a tetrahedron, though not very large, are real. At this stage we merely note their existance, without trying to discover their physical meaning.

Because of this effect, differences *between* tetrahedra cannot be regarded as real unless they are significantly greater than the average differences *within* tetrahedra. Thus significance tests for tetrahedral means must be based on comparisons of differences with $\varepsilon(r)$ rather than with $\sigma(r)$.

It is next necessary to consider whether the mean radii of tetrahedra in the same group differ significantly from one another. From Table 3 (2) it can be seen that the differences are not significant. If the test had been carried out using $\sigma(r)$ in place of $\varepsilon(r)$, the ratios would have been 7 and 4 respectively, indicating high significance. Thus we can say that, while the differences between tetrahedral means are real, they are only of the order of magnitude of differences within tetrahedra, and therefore cannot be used as evidence for different Si/Al ratios in the atoms occupying them.

By contrast, we may apply the same test, using $\varepsilon(r)$, to the difference between the group means (Table 3 (3)). This difference is seen to be highly significant.

We now use the results of Smith (1954) to examine the Si/Al ratios corresponding to the group mean bond lengths. Smith's values are $1{\cdot}60\pm0{\cdot}01$ Å for Si–O, $1{\cdot}78\pm0{\cdot}02$ Å for Al–O, and it would be reasonable to assume, for statistical study, that his estimated errors are about twice the standard deviation. However, Smith (1960) expresses doubt about the constancy of the bond lengths within these limits in all circumstances. To make some allowance for this, we use the estimated errors as if they were s.d.'s.

Table 3. *Significance of bond-length differences*

Key to symbols:

r_t = tetrahedral mean bond length
r_g = group mean bond length
r_{Sm} = Smith's empirical bond length
$\varepsilon(r)$ = r.m.s. deviation of single bond length
$\sigma(r)$ = s.d. of single bond length calculated from $\sigma(x_n)$
$\Delta(r)$ = Smith's estimated limit of error

	Quantities compared	σ	δl	Set of tetrahedra	Numerator	Denominator	Cruickshank ratio	Significance*
(1)	Single bond	$\sigma(r)$	$\varepsilon(r)$	(i) Small	0·024 Å	0·0044 Å	5·5	High
	Tetrahedral mean	$\sigma(r)/2$		(ii) Large	0·031	0·0044	7	High
(2)	Tetrahedral mean	$\varepsilon(r)/2$	$\lvert(r_g-r_t)_{\max.}\rvert$	(i) Small	0·014	0·013	1·1	Zero
	Group mean	$\varepsilon(r)/2\sqrt{8}$		(ii) Large	0·009	0·016	0·6	Zero
(3)	Group mean, small	$\varepsilon_{Si}(r)/2\sqrt{8}$	$\lvert(r_g)_{Si}-(r_g)_{Al}\rvert$	All	0·035	0·007	5	High
	Group mean, large	$\varepsilon_{Al}(r)/2\sqrt{8}$						
(4)	Smith's bond length	$\Delta(r)$	$\lvert r_g-r_{Sm}\rvert$	(i) Small	0·014	0·011	1·3	Zero
	Group mean	$\varepsilon(r)/2\sqrt{8}$		(ii) Large	0·031	0·041	1·5	Zero

* Significance levels are those suggested by Cruickshank (1949): 'high' and 'zero' correspond to probabilities of accidental occurrence of $<0{\cdot}1\%$ and $>5\%$ respectively, or $\delta l/\sigma > 3{\cdot}1$ and $< 1{\cdot}65$.

Then from Table 3 (4) it can be seen that the differences of the group means from Smith's values for pure Si and pure Al are not significant. It is true, of course, that no significance test is more objective or carries more weight than the postulates on which it is based; however, it is certainly clear that there is no evidence from which we can reliably deduce any departure from perfect Si/Al order.

It is perhaps worth noting that, from Smith's values, one would deduce the presence of 8% Al in the Si-rich sites, 17% Si in the Al-rich sites. In view of the particular difficulty experienced by Smith in fixing the Al end of his scale, the latter estimate is quite unreliable.

It is interesting that in both forms of $BaAl_2Si_2O_8$, the felspar celsian (Newnham & Megaw, 1960) and the non-felspar paracelsian (Bakakin & Belov, 1960), there is also a high degree of Si/Al order, and no certain evidence that order is less than perfect (though neither structure is so far refined as anorthite). In celsian, the pattern of Si-rich and Al-rich sites is the same as in anorthite.

Inspection of Table 2(*c*) suggests that the tetrahedral means in anorthite differ *less* from the group mean than would be expected from their variations within a tetrahedron if the tetrahedra provided random samples. This may be tested by comparing the two estimates of the standard deviation of the group mean, namely [r.m.s. value of $\varepsilon(r)$]/$\sqrt{(32)}$ and (r.m.s. value of (r_t - group mean)]/$\sqrt{8}$. From Table 2(*c*) these are $0{\cdot}0043 \pm 0{\cdot}0006$ Å, $0{\cdot}0029 \pm 0{\cdot}0007$ Å respectively for Si–O; $0{\cdot}0055 \pm 0{\cdot}00035$ Å, $0{\cdot}0018 \pm 0{\cdot}00029$ Å respectively for Al–O. The Cruickshank ratios are therefore 1·6 for Si–O, 8 for Al–O, indicating doubtful significance for the former, high significance for the latter. Non-randomness could be caused by the pseudo-symmetry discussed later (§ 3·3), but its more conspicuous manifestation for Al–O is rather striking: it suggests that the *volume* occupied by an Al atom is more nearly constant than would be expected if it were controlled purely by the direct Al–O contacts.

The largest Si-rich tetrahedral mean in anorthite, 1·628 Å, is not far from the $Si_2(m)$–O tetrahedral mean in reedmergnerite, $NaBSi_3O_8$, (Clark & Appleman, 1960) which has the value 1·623 Å. In reedmergnerite (which has the felspar structure) there is no possibility of attributing the large value to Al substitution. This supports the conclusion previously reached that it is unsafe to do so in anorthite.

The results of this section may be summed up by saying that the structure contains a regular alternation of Si and Al tetrahedra, such that any O atom has one Si neighbour and one Al; that the ordering of Si and Al is perfect, within the limits of experimental error (which suggest that disorder is in any case less than 10%); that the individual bond lengths within tetrahedra vary slightly, but that the tetrahedral means are rather more uniform than would have been expected if the individual variations were wholly random.

2·2. *Environment of* Ca

Since there are four different subcells, there are four differently situated Ca atoms. The Ca–O distances are listed in Table 2(*a*), the seven shortest for each Ca on the left-hand side of the column, other distances of less than 4 Å on the right. The distances on the left-hand side include all up to 3·1 Å, and the O atoms concerned may be counted as neighbours; each Ca is then 7-coordinated. One of these distances, however, —the O_C bond of Ca(000)—is so much longer that any of the others that it might have more meaning physically to count it as a non-bonding contact, and take this Ca as 6-coordinated. No arguments depend critically on which choice is made; indeed with irregularly coordinated atoms like Ca there is not much significance attached to any such choice.

All other bonds are within the usual range for Ca–O, except that from Ca(000) to $O_A(2)$, which is exceptionally short. Bonds from cation to $O_A(2)$ tend to be

short in most felspars, and in anorthite the $O_A(2)$ bonds of the other three Ca's are also short.

It can be seen that the configurations round Ca($z0c$) and Ca($0ic$) resemble one another very closely; Ca(000) and Ca($zi0$), though not quite so much alike, nevertheless resemble each other much more than they do the other Ca's.

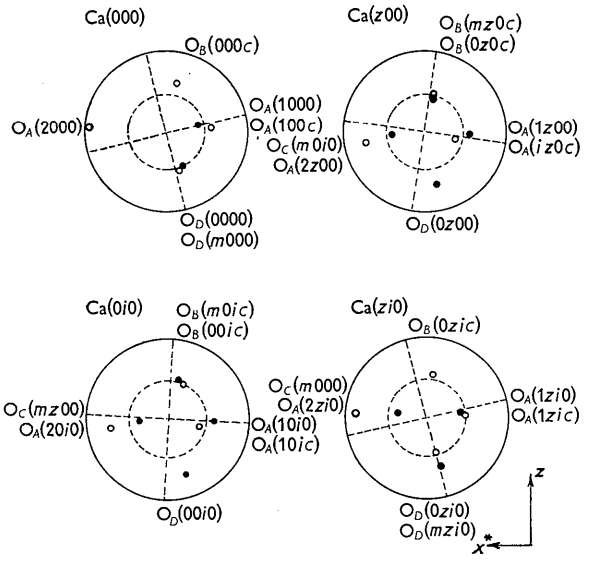

Fig. 2. Stereograms of environment of the four Ca atoms. Intersections of the small circles and diameters shown with dashed lines are at the corners of a regular cube. Where the symbols of two atoms are written together the upper symbol refers to the atom in the upper hemisphere.

Stereograms showing the directions of the Ca–O bonds are given in Fig. 2. (Note that the groups related by subscript c are related by a true centre of symmetry; it is more convenient here to consider Ca($z00$) and Ca($0i0$) than the equivalent (Ca($z0c$) and Ca($0ic$)). The general resemblance of the coordination to a distorted cube with one corner missing (or two corners for Ca(000), if this is taken as 6-coordinated) can be seen. In more detail, one may note that four bonds (to two $O_A(1)$ and two O_B *or* two O_D atoms) approximate rather closely to cube-corner directions, the bond to $O_A(2)$ lies roughly along the bisector of the angle between the two $O_A(1)$ bonds, and the other toms fait in as best they can. It is as if the steric necessity to fit the $O_A(2)$ atom in this direction, at a rather short distance, upset the regular angular arrangement of the neighbouring O's.

It is often said that the large cations in a felspar are situated in a 'cavity' in the Si/Al–O framework. This suggests that they are perhaps rather loosely held in place, or that there may be more than one possible position for them. It is true that there is a large cavity enclosed by 10 oxygen atoms, but in anorthite the corrugations of its walls are such as to grip each Ca atom tightly. This central interstice has two essentially different shapes, one bounded by two O_B's and one O_D, one by one O_B and two O_D's. If the coordinates of Ca in one such interstice are altered by $z=\frac{1}{2}$, it will not fit into the other interstice; one of the distances to O_B or O_D is impossibly short. The same is true of any other such interchanges (cf. Table 4).

The isotropic B value of about 1·0 Å^2 is comparable with that found for the cation in other felspars; the accuracy with which it or its anisotropy is determined is not great enough to draw elaborate conclusions. It is certainly larger than for the other atoms. Whether it represents a true thermal vibration of r.m.s. amplitude about 0·1 Å, or a random distribution of Ca atoms within about 0·1 Å of a mean position (which might result from 'frozen-in' thermal amplitudes), cannot be decided on present evidence. Outside these limits, there is no evidence for Ca disorder, and any displacement of Ca would need corresponding changes in the shape of the framework to make room for it.

Table 4. *Bond lengths (in* Å*) with* Ca *placed at 'right' and 'wrong' sites in subcell*

(A 'wrong' site is one derived by adding ½ to all the coordinates of a Ca atom whose symbol differs by i from that of the right atom for the subcell)

	Subcell 00		Subcell $z0$		Subcell $0i$		Subcell zi	
Neighbours	Right Ca(00)	Wrong Ca($0i$)	Right Ca($z0$)	Wrong Ca(zi)	Right Ca($0i$)	Wrong Ca(00)	Right Ca(zi)	Wrong Ca($z0$)
$O_A(1)$	2·62	*2·19*	2·48	2·65	2·46	2·85	2·47	*2·30*
$O_A(1)$	2·50		2·72	2·41	2·82	*2·28*	2·59	2·87
$O_A(2)$	2·28	2·34	2·35	2·31	2·34	2·31	2·32	2·35
O_B	2·37	*2·27*	2·46	2·63	2·41	2·60	2·42	*2·30*
O_B		2·92	2·49		2·50			2·72
O_C	(3·09)	2·61	2·57	2·87	2·57		2·81	2·50
O_C								
O_D	2·42	2·68	2·40	*2·16*	2·38	*2·17*	2·39	2·67
O_D	2·53					2·93	2·77	

(Ca–O bond lengths of 2·30 Å and less are regarded as too short to be stable unless in exceptional cases, e.g. the bond to $O_A(2)$ which is abnormally short in most felspars. Unsatisfactory values are shown in italics.)

Table 5. *Electrostatic valence*

	O atoms in group	No. of Ca neighbours	Electrostatic valence
Group 1	$O_A(100)$, $O_A(10i)$, $O_A(1z0)$, $O_A(1zi)$ (4 altogether)	2	2·32
Group 2	$O_A(200)$, $O_A(20i)$, $O_A(2z0)$, $O_A(2zi)$, $O_B(000)$, $O_B(00i)$, $O_B(0z0)$, $O_B(0zi)$, $O_B(m0i)$, $O_B(mz0)$, $O_C(0zi)$, $O_C(m00)$, $O_C(m0i)$, $O_C(mz0)$, $O_D(000)$, $O_D(00i)$, $O_D(0z0)$, $O_D(0zi)$, $O_D(m00)$, $O_D(mzi)$ (20 altogether)	1	2·04
Group 3	$O_B(m00)$, $O_B(mzi)$, $O_C(000)$, $O_C(00i)$, $O_C(0z0)$, $O_C(mzi)$, $O_D(m0i)$, $O_D(mz0)$ (8 altogether)	0	1·75

Table 6. *Bond angles at oxygen in various felspars*

Angles are given in degrees, rounded off to the nearest degree
Where independent values are taken together in a group, the extreme values are recorded, and also (in brackets) the mean of the group

	Microcline	Low albite	High albite	Orthoclase	Celsian	Anorthite
$O_A(1)$	144	142	144	144	139	(137) 135–140
$O_A(2)$	140	131	133	139	135	(124) 122–126
O_B	(153) 152–155	(150) 140–160	(149) 142–155	153	(150) 150	(144) 128–171
O_C	(131) 130–132	(130) 125–135	(131) 128–134	131	(129) 127–130	(131) 128–133
O_D	(142) 140–144	(141) 134–147	(140) 136–144	142	(139) 138–139	(141) 125–167

2·3. O–O *distances, and bond angles at* Si *and* Al

These are recorded in Table 2(*d*), (*e*), and (*f*). Since the standard error in the determination of bond angle is about 0·5°, the difference of the angles from the tetrahedral value are real; their structural significance will be left for discussion in § 3·3.

2·4. *Environment of* O *atoms, and bond angles at* O

Each O atom has one Si neighbour and one Al; the angle between these two bonds is recorded in Table 2(*g*). In addition, many of the O's have Ca neighbours: each $O_A(1)$ has two, as in other felspars, and most other O's have one, but certain O's have none within what are regarded as effective bonding distances. Table 5 shows the symbols of the atoms in each group, and their electrostatic valence. (Here Ca(000) is counted as 7-coordinated; the effect of counting it as 6-coordinated would be to transfer $O_C(0zi)$ from group 2 to group 3, with negligible effect on any of the arguments for which this classification is later used).

The bond angles at O resemble in a general way those in other felspars (Table 6), but on the whole show a larger spread of values. They are of the order of magnitude of those found in other silicates (cf. Liebau, 1960). Detailed discussion is left to § 3·3.

The average temperature factor for O has a B-value of 0·6 Å^2 (Paper I). This, though not very accurately determined, is still appreciably lower than the values found in some other felspars (Table 7). It is an indication that we are here dealing with an ordered structure, and that the O atoms are not spread over a wide range of neighbouring positions in different unit cells, as

Table 7. *Isotropic B values in* Å^2

	Microcline	Low albite	Sanidine	Orthoclase	Celsian	Anorthite	Reedmergnerite
Large cation	1·0	1·3	1·9	1·0–1·5	0·5–1·2	0·3–1·0	1·23
T	—	—	—	0·6	0·6*	0·2	0·33†
O	—	—	—	1·2	1·2*	0·6	0·67†

* These figures refer to the penultimate stage of refinement, when the structure was still being treated as if there were complete Si/Al disorder. No revised estimates were made at the later stage.

† Information kindly supplied by Dr D. E. Appleman, 1962.

must inevitably happen if Si and Al are distributed at random in the tetrahedral sites, because of their difference of radii.

3. Discussion

3·1. *Concept of structure as a framework built from elastic 'building elements'*

There is much to be gained from a consideration of the anorthite structure as if it were a construction built on engineering principles, according to the macroscopic laws of statics. We first consider the Si/Al–O framework, neglecting the large cation. Suppose all Si–O and Al–O bonds are rigid rods with lengths of 1·61 units and 1·75 units respectively, all angles at Si and Al are exactly tetrahedral, and all angles at O exactly 130°; O–O contacts, between different tetrahedra, of less than 2·7 Å are forbidden. Attempts to build a structure resembling that of felspars, and repeating itself with a parallelepiped of approximately $8 \times 13 \times 7$ units, will probably show that it cannot be done. We must endow our building elements with elasticity—the rod lengths with a Young's modulus, the hinge angles with a rigidity modulus. It may then prove possible to build the required periodic structure. The existence of the felspars proves that it *is* possible but suggests also that the structure will not be in stable equilibrium (in the sense used in statics) unless it is propped open with spacers of appropriate size, namely spheres of radius about 1 to 1·3 units. If the role of the large cation were merely to maintain electrical neutrality we should expect to find felspars in which magnesium, and possibly beryllium and lithium, could play this part. As it is, the hinged framework shears till the forces due to elastic compression of the spacer are called into play, and, when the spacer is large enough, equilibrium results. In determining the detailed nature of the shear, the electrostatic forces play their part.

In this process, all the bond lengths and bond angles are necessarily strained from their ideal values; the amount of strain adjusts itself at each, so that over the structure as a whole the energy is a minimum. Thus there are intrinsic strains in the various building elements when the structure as a whole has its equilibrium configuration.

Assuming a knowledge of the unstrained dimensions of the building units and their elastic constants, and a Hooke's law relation between stress and strain, one could in theory set up equations from which to derive the equilibrium configuration and all individual strains. In practice the mathematical solution of the equations might be too difficult. For a crystal structure there are the further difficulties (i) that we do not know our unstrained lengths and angles, because they never exist in isolation, (ii) that we cannot be sure of the validity of a Hooke's law approximation, and (iii) that the elastic constants themselves may depend on such influences as the electrostatic field of neighbouring atoms. Nevertheless an empirical examination of bond lengths and angles along these lines, taking the strains as deviations from the best estimated mean value, provides a useful starting point.

It turns out that the model needs to be adapted to allow for electrostatic attractive and repulsive forces emanating from the large cations, as well as the homopolar (or semipolar) attractive forces in the framework, and the repulsive forces within the framework and between cation and oxygen. These will be considered in more detail later.

3·2. *Framework and 'lattice' vibrations*

This girder-type model enables us to understand the doubling of the unit cell additional to that required by the Si/Al alternation. If all bond lengths and bond angles are strained in order to achieve a periodic repeat, doubling the period doubles the numbers of atoms over which the strain is to be distributed, and therefore (roughly) halves the individual strains with a consequent reduction in strain energy.

One may then ask why, if longer periods lower the strain energy, periodic structures are ever achieved? The answer lies in the fact that we have so far considered only potential energy. An actual macroscopic structure has natural frequencies corresponding to modes of vibration, and kinetic energies associated with them. The corresponding features of the crystal structure are the 'lattice vibrations' and their contribution to the free energy. Presumably this part of the energy is so much less for a periodic structure that it more than compensates for the extra strain energy. It is, however, temperature-dependent; and a transition to a structure of half the period at higher temperatures could be caused by a changing distribution of energies between the available vibration modes in a way which favoured shorter wave lengths.

The very small variations in Si–O bond lengths, and the only slightly larger variations in Al–O, show that these bonds are elastically stiff; by comparison the Ca–O bonds are elastically compliant. A similar contrast is seen for Si and Al bond angles on the one hand, Ca bond angles on the other. It is therefore to be expected that the Si/Al–O framework will vibrate as a whole, in 'lattice' modes, while Ca will vibrate more nearly independently, in Einstein modes. (This is perhaps a crude approximation, but it is only intended to give a qualitative picture). Since the force constants of the Ca–O bonds are smaller than of bonds and angles in the framework, and the effective mass concerned in the framework vibrations is greater than that of a single Si/Al or O atom, the vibration amplitudes of Ca are likely to be larger than those of Si/Al or O. This agrees with the observations of B values in anorthite, and also in reedmergnerite, the only other perfectly ordered structure for which detailed information is available.

Again, since the spread of values of bond angles

at O suggests that such angles are elastically more compliant than those at Si and Al, and since moreover the greater mass of Si/Al compared with O might tend to make them act as nodes for the standing waves, it is reasonable to expect that Si/Al amplitudes should be still less than O-amplitudes. This is observed. It may be related to the smaller difference parameters of T atoms compared with O atoms (Paper I, Table 5 and Table 9), as if the T atoms tended to stay as fixed points during the distortions of the parts of the structure round them. The B values recorded for other felspars are in accordance with these ideas (cf. Table 7); but when Si/Al disorder is believed to be present in the structure (as in the simplest interpretation of orthoclase) or is simulated by an averaging process at the stage at which the B values are computed (as was true of celsian, and is a possible interpretation of orthoclase) care has to be taken in estimating the effects of thermal vibration, because the experimental evidence does not distinguish between this and disorder broadening of the peaks. It is therefore rather surprising that in both orthoclase and celsian the B values for Si/Al are so low; it is obviously due to the same physical cause as the small size of the difference of T coordinates in anorthite. In both orthoclase and celsian the disorder broadening is manifested in B values for oxygen which are much larger than those in the ordered structures. For the A cations, if the very large anisotropy in the albites is attributed to disorder, and the smaller anisotropy in some of the others is ignored, all have isotropic B values of about 1 to 2 Å.

3·3. *Detailed examination of intrinsic strains*

We proceed to examine the intrinsic strains of individual bond lengths and bond angles, to see what regularities can be noted and how far they can be correlated with each other or with physically reasonable causes.

(i) *Bond angles at* O

Since, of all the 'building elements' of the structure, these show the greatest spread, and are therefore most compliant, it is convenient to consider them first.

Table 2(g) shows that a classification according to the type of atom ($A(1)$, $A(2)$, B, C, or D) is a natural one for demonstrating regularities. At O_C, the angles are all closely alike ($\sim 130°$), not only in anorthite but in other felspars (Table 6). There is similar consistency at $O_A(1)$, with slightly lower values ($\sim 138°$) for the 14 Å felspars than for the 7 Å felspars ($\sim 143°$). At $O_A(2)$ the angles in anorthite are even more consistent as a group, but conspicuously lower than in any other felspar. At O_B and O_D there is much more spread in all felspars, and in anorthite it is so great that there is not much significance in recording the mean.

The O_B and O_D atoms at which very large angles (160–170°) occur are those which have no Ca neighbour. At first glance one might try to correlate large angles with low electrostatic valence. This, however, cannot be substantiated by consideration of the other O bond angles, since comparison with Table 5 shows that (a) high values of electrostatic valence at $O_A(1)$ are associated with normal bond angles, and normal values at $O_A(2)$ with low bond angles, (b) similar values at $O_A(2)$ and half the O_C's are associated with different bond angles, (c) different values for two sets of O_C's are associated with similar bond angles. These qualitative comparisons can be substantiated by detailed statistics. It must be concluded either that the electrostatic field does not play a large part in controlling the bond angles or that the simple treatment of the field embodied in the Pauling rules for electrostatic valence is inadequate for evaluating its effect on bond angle.

In fact it seems much more likely that steric effects (depending on repulsive forces) play the main part in determining the oxygen bond-angle strains. One piece of supporting evidence is the fact that abnormally high angles at some O_B, O_D sites are compensated by low values at others within the same ring of four linked tetrahedra, so that the means for each ring are very much alike (Table 8). It is very noticeable that, for these angles as for the Ca environments, the closest resemblance among the four subcells is between those related by the base-centring operation zi. This point will be considered further below.

(ii) Si–O *and* Al–O *bond lengths*

The grouping of bond lengths to show up regularities in their strains may be tried in three ways, as follows (grouping into tetrahedral means having been shown to smooth out differences rather than emphasize them). The first way is according to the number of Ca neighbours of the O atom, as given in Table 5. The results are shown in Table 9. There is obviously a significant shortening for group 3 as compared with group 2; between groups 1 and 2 the differences for Si and Al separately are not (formally) significant,

Table 8. *Bond angles (in degrees) in the four different* O_B–O_D *rings*

Atom	Angle	Atom	Angle	Atom	Angle	Atom	Angle
$O_B(0000)$	129·4	$O_B(mzi0)$	163·6	$O_B(0z00)$	139·6	$O_B(m0i0)$	145·3
$O_D(0000)$	137·8	$O_D(mzi0)$	138·5	$O_D(0z00)$	125·2	$O_D(m0i0)$	166·9
$O_B(mz0c)$	143·5	$O_B(00ic)$	135·9	$O_B(m00c)$	170·8	$O_B(0zic)$	128·3
$O_D(mz0c)$	161·4	$O_D(00ic)$	124·6	$O_D(m00c)$	140·3	$O_D(0zic)$	132·6
Mean	143·0	Mean	140·6	Mean	144·0	Mean	143·8

Table 9

(*a*) Comparison of *T*–O bonds according to environment of O

	No. of Ca neighbours	Mean bond length		S.d. of mean bond length	
		Si–O	Al–O	Si–O	Al–O
Group 1	2	1·632 Å	1·780 Å	0·007 Å	0·015 Å
Group 2	1	1·622	1·755	0·005	0·006
Group 3	0	1·588	1·719	0·008	0·009

(*b*) Significance tests

		Group 1–2	Group 2–3
Cruickshank significance ratio c_s	Si	$10/(7^2+5^2)^{\frac{1}{2}} = 1{\cdot}16$	$34/(5^2+8^2)^{\frac{1}{2}} = 3{\cdot}62$
	Al	$25/(15^2+6^2)^{\frac{1}{2}} = 1{\cdot}56$	$36/(6^2+9^2)^{\frac{1}{2}} = 3{\cdot}33$
Probability of accidental occurrence of observed difference*	Si	0·12	< 0·001
	Al	0·06	< 0·001
	Joint	0·007	$< 10^{-6}$

* Calculated from Cruickshank's expression, $P = \frac{1}{2} - \frac{1}{2}\,\mathrm{erf}\,(c_s/\sqrt{2})$.

but since the probability for their joint occurrence accidentally is the product of the separate probabilities, the combined effect is significant. (Errors in the coordinates of any O, which would affect both its bonds, would tend to do so in opposite directions, because the bond angle is greater than 90°; hence they could not give rise to systematic differences in the same direction between both kinds of bonds).

The second way of grouping bonds is according to the type of O atom, which proved effective for O bond angles. Average values for both kinds of bonds involving $O_A(1)$ are slightly larger than for those involving $O_A(2)$, and these again than for bonds involving O_B, O_C, O_D, which show no consistent trend; but none of the differences is large enough to be significant. Bonds to $O_A(2)$, which is linked by the abnormally short bond to Ca, are if anything longer than normal; hence the shortening of Ca–$O_A(2)$ is not due to stresses exerted on $O_A(2)$ by its *T* neighbours.

The third way is a comparison of *T*–O bond lengths with bond angle at O. This showed no detectable regularity, except what could be accounted for by the fact that the four atoms with largest angle have no Ca neighbour.

It therefore seems clear that the most conspicuous differences of Si–O and Al–O bond length depend on the number of Ca neighbours of the O atom. Such an effect has been suspected previously, e.g. by Smith (1960), Smith, Karle, Hauptman & Karle (1960), Radoslovich (1960); but is here conclusively demonstrated. It means *either* that there are intrinsic stresses in the *T*–O bonds due to the stresses applied to them by the Ca–O bonds, *or* that the electrostatic field of Ca acts directly on the bonds to lengthen them. Which explanation is physically more realistic cannot be decided on this evidence.

It also remains doubtful which of the lengths should be regarded as 'unstrained', since there are certainly other stresses operating besides those in the Ca–O bonds—notably those affecting the bond angles at O. It is not surprising, for example, that Si–O bonds in this structure for O atoms with no Ca neighbours should be shorter than in a structure such as quartz where *none* of the O's has any other neighbour.

No similar effects have been observed with certainty in other felspars. For intermediate microcline, orthoclase and celsian, the scatter of individual bond lengths within a tetrahedron is insignificant ($\varepsilon(r) \sim 0{\cdot}005$ Å or less). For low albite, the scatter is rather large ($\varepsilon(r) = 0{\cdot}021$ Å) but so is the standard error of determination ($\sigma = 0{\cdot}019$ Å). For high albite, with about the same σ, the scatter is small (0·008 Å). For reedmergnerite, $NaBSi_3O_8$ (with the felspar structure), the scatter is rather larger in proportion ($\varepsilon(r) = 0{\cdot}017$ Å, $\sigma = 0{\cdot}010$ Å), which suggests that the deviations are real; but the margin is too narrow to allow very definite conclusions. More detailed information from three-dimensional analysis of the albites is desirable.

(iii) *Bond angles at* Si *and* Al

Inspection of Table 2(*f*) suggests some degree of uniformity within groups of four tetrahedra. Accordingly, bond-angle strains (differences from the tetrahedral angle, 109·5°) for corresponding angles were averaged over the four atoms whose symbols are derived from any one of the set by operations 000, 00*i*, *m*00, *m*0*i*—i.e. for atoms related topologically (not exactly) by body-centring and mirror-plane operations. The results (Table 10) show clearly that corresponding angles for different atoms within a set have on the average very small differences from one another as compared with the differences between their means. (Most of these differences are large compared with the estimated experimental error, $\sim 0{\cdot}5°$). Moreover, while T_1 and T_2 tetrahedra show quite different sets of strains, tetrahedra containing Si or Al respectively (related by operator *z*) have very similar strains, except that those for Al are slightly (perhaps not significantly) larger.

Table 10. *Bond angle strains (in degrees) and* O–O *tetrahedron edge strains (in* Å)

Strains are deviations from values for a regular tetrahedron
The table lists the means over corresponding angles and edges in similar tetrahedra, and their standard deviations

Type of tetrahedron	O atoms	O–O edge in anorthite		O–*T*–O angle												
				Anorthite		Low albite		High albite	Microcline		Orthoclase		Sanidine	Celsian		
		Si	Al	Si	Al	Si	Al	Si/Al	Si	Al	Si	Si/Al	Si/Al	Si	Al	
T_1	*AB*	−0·105	−0·148	−6·9	−8·4	−3·9	−5·9	−4·8	−4·8	−2·2		−3·4	−4·2	−6·5	−6·9	
		±0·020	±0·004	±1·3	+2·1			±0·3								
	AC	+0·091	+0·113	+5·9	+6·7	+3·7	+5·6	+2·5	+3·5	+3·7		+5·1	+3·5	+6·7	+6·4	
		±0·015	±0·027	±1·2	±1·7			±0·6								
	AD	−0·094	−0·138	−6·2	−8·5	−2·9	−6·2	−4·6	−4·3	−2·8		−3·4	−3·4	−6·5	−8·4	
		±0·009	±0·031	±0·9	±2·5			±1·0								
	BC	+0·021	+0·024	+2·1	+3·1	−0·6	+2·1	−1·5	+3·2	+0·7		+0·7	+1·4	+1·8	+4·1	
		±0·012	±0·019	±0·8	±0·7			±3·5								
	BD	+0·058	+0·075	+3·8	+4·9	+1·2	+0·7	+3·0	+0·2	+0·1		+0·5	+2·4	+4·2	+4·3	
		±0·012	±0·038	±1·1	±1·2			±4·0								
	CD	−0·002	+0·005	+0·8	+1·6	+0·8	+2·6	+4·5	+0·9	−4·8		−0·7	−0·3	+0·1	−0·5	
		±0·032	±0·022	±1·0	±0·5			±1·7								
T_2	*AB*	−0·005	−0·046	−0·4	−2·8	−1·1		−2·9	−1·0		+0·6		+0·6	−3·1	−3·0	
		±0·020	±0·040	±1·6	±2·3	±1·5		±1·7	±0·4							
	AC	−0·090	−0·110	−5·9	−6·2	−5·0		−2·5	−4·3		−4·9		−4·9	−6·2	−8·4	
		±0·019	±0·019	±1·0	±1·3	±0·9		±0·1	±0·3							
	AD	+0·011	−0·053	+0·9	−3·1	−1·5		−2·2	−0·9		−0·8		−0·6	−0·6	−0·6	
		±0·004	±0·018	±0·7	±1·2	±0·7		±1·3	±0·2							
	BC	+0·034	+0·026	+2·5	+2·3	+3·5		−1·8	+1·2		+1·8		+0·4	+4·0	+3·3	
		±0·031	±0·024	±0·7	±0·8	±0·5		±2·3	±0·2							
	BD	−0·038	+0·033	−1·2	+2·4	+1·0		+1·3	+1·2		+1·6		+2·1	+2·3	+3·3	
		±0·030	±0·017	±1·5	±0·9	±0·3		±0·4	±0·2							
	CD	+0·046	+0·089	+3·6	+6·2	+2·1		+7·4	+3·3		+1·3		+2·3	+2·9	+4·3	
		±0·015	±0·018	±0·7	±1·0	±1·7		±0·2	±0·9							

Exactly similar effects are shown by an analysis of the O–O bond-length strains, i.e. the differences from the values 2·640, 2·860 Å, corresponding to regular tetrahedra with T–O distances 1·614, 1·749 Å respectively. These are also shown in Table 10. The consistent differences between the edges $T_1(AC)$ and $T_2(AC)$ in a number of felspars was earlier noted by Jones & Taylor (1961), who pointed out that it could not be due to a difference in Si/Al ordering but must 'be due to the general balance of forces as between Si/Al and O on the one hand, and K (or Ba) on the other.'

The more detailed analysis of the present paper allows us to go further. Table 2(f), or its analysis in Table 10, shows that in anorthite all tetrahedra of the same type (T_1 or T_2) tend to have the same shape, i.e. the same angular strains, whatever their position or orientation in the structure, and whatever the nature of T. These tetrahedra are not related by symmetry, though of course their general arrangement is not far from the symmetrical sanidine structure. It therefore seems that the strains, and consequently the stresses producing them, are not on the whole very sensitive to the detailed coordinates of the atoms and their departure from the higher symmetry. (In so far as bond-length strains may be associated with any of the same regularities as affect bond-angle strains, similarity between tetrahedra of the same type will have the effect of making their T–O tetrahedral means more nearly alike than would have been expected from a random distribution of the bond lengths throughout the structure, thus tending to explain the observation noted in § 2·1.)

Some striking facts emerge from comparison of the bond angles with those in other felspars (Table 10). The largest strains, those in $T_1(AB)$, $T_1(AC)$, $T_1(AD)$, $T_2(AC)$, are observed in *all* the felspars studied; they do not vary greatly within a structure, and the mean value of each for a given structure is roughly constant for all the felspars with cations of similar valency (Table 11), the ratio of the strains for divalent and monovalent cations being about 1·7. The strains must therefore be due (like the T–O bond-length elongations) to the effect of the A cations. The stresses causing them must, like the strains, be relatively insensitive to small differences in atomic coordinates and configuration round A. Since the A atom is nearly on a mirror plane of symmetry, and is nearly repeated by a body-centring translation, this explains the close resemblance in shape between different tetrahedra in the same structure as well as between different structures. The relative insensitivity of the strain to the departure from overall monoclinic symmetry is particularly striking: the monoclinic (or nearly monoclinic) potassium felspars are only slightly different from the distinctly triclinic albites, but quite different from monoclinic celsian.

3·4. *Bond-angle strain as a consequence of electrostatic repulsion*

The mechanism by which the cation affects the O–T–O bond angle must be treated in terms of electrostatic forces, because even if homopolar forces contribute to the Ca–O bond we have no means of estimating them. As a nearest-neighbour effect, the electrostatic field of Ca polarizes each neighbouring O and thereby influences both the attractive and repulsive forces between O and its other neighbours. For second-nearest-neighbour effects, we must consider Ca–Ca and Ca–T electrostatic repulsions; this looks formidable at first glance but is greatly simplified if one recognizes the shielding of Ca by its surrounding O's. Since these are polarizable, one may represent them in a crude model by conducting spheres of radius about 1·5 Å. For this purpose one must include *all* O's at distances not greater than the cation–cation distances to be studied, since it is not merely O's in contact with Ca which serve to shield it. Then only where there are gaps in the shell of O's is cation–cation repulsion likely to be important. This effect can be visualized using lines of force. The ideas used here are the same as those underlying Pauling's electrostatic-valence concept.

Table 11. *Comparison of bond angles showing large strain: mean values over all similar tetrahedra*

Large cation	Felspar	Mean bond-angle strain (degrees)			
		$T_1(AB)$	$T_1(AC)$	$T_1(AD)$	$T_2(AC)$
Na^+	Low albite	−4·9	+4·6	−4·6	−5·0
Na^+	High albite	−4·8	+2·5	−4·6	−2·5
K^+	Microcline	−3·5	+3·6	−3·5	−4·3
K^+	Orthoclase	−3·4	+5·1	−3·4	−4·9
K^+	Sanidine	−4·2	+3·5	−3·4	−4·9
Ca^{++}	Anorthite	−7·7	+6·3	−7·3	−6·1
Ba^{++}	Celsian	−6·7	+6·5	−7·5	−7·3
1-valent	Mean	−4·2 ±0·3	+3·9 ±0·4	−3·9 ±0·3	−4·3 ±0·4
2-valent	Mean	−7·2 ±0·4	+6·4 ±0·1	−7·4 ±0·1	−6·7 ±0·4
Ratio $\frac{2-\text{valent}}{1-\text{valent}}$		1·7	1·6	1·9	1·6

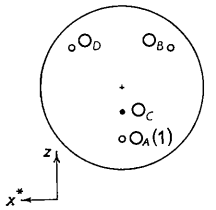

Fig. 3. Sketch stereogram of the environment of $T_1(0000)$.

The fact that the largest O–T–O strains are those involving the three angles round T_1–$O_A(1)$ is sufficiently striking to provide an empirical starting point for study. The geometrical consequence of these strains can be seen from Fig. 3. As compared with a regular tetrahedron, angles AB and AD are too small, AC too large; in other words, T–$O_A(1)$ is tilted further downwards. To restore regularity, it would be necessary to increase the y coordinate of $O_A(1)$, and hence (because of the centre of symmetry and pseudo-symmetry axis) to increase the edge $O_A(1)$–$O_A(1)$ and the bond angle at $O_A(1)$. The latter is already slightly too large (135° instead of the unstrained 130°), but in view of the softness (high compliance) of T–O–T angles, further changes are hardly likely to give prohibitive energy increase. On the other hand, $O_A(1)$–$O_A(1)$ is a shared edge between two Ca polyhedra; its length, ~3·2 Å, is also rather high for such an edge. It seems that there are strong forces tending to make it contract.

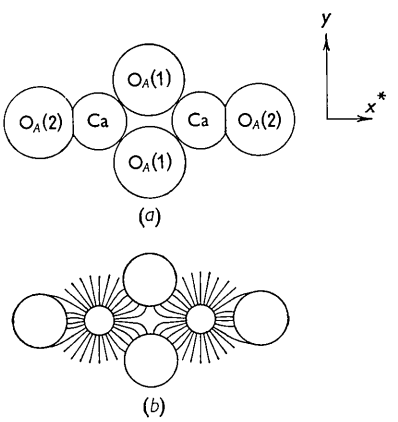

Fig. 4. Environment of a pair of Ca atoms related by a centre of symmetry; section in plane perpendicular to [001]. (*a*) Packing diagram, with radii drawn to scale; (*b*) lines of force, with atomic centres as in (*a*), but radii reduced to show effect more clearly.

The electrostatic origin of the forces tending to shorten $O_A(1)$–$O_A(1)$ can be shown as follows. The shielding shell of Ca comprises ten O's (two each of $O_A(1)$, $O_A(2)$, O_B, O_C, O_D). The only serious gap in it is at the edge $O_A(1)$–$O_A(1)$, across which there is another Ca at a distance of about 4 Å. Fig. 4(*a*) shows a section in a plane perpendicular to [001], drawn approximately to scale. The abnormally short Ca–O distance is shown by the cut-off of the circles at a common chord. Assuming the $O_A(2)$–$O_A(2)$ distance to be fixed by other parts of the framework not shown (cf. below, § 4·1), the Ca–O distances could be made more nearly normal by moving the Ca's nearer together and the $O_A(1)$'s further apart, thus relieving the strain in the angles at T_1 and $O_A(1)$ also. But the Ca's are kept apart by their electrostatic repulsion, and this also draws together the two $O_A(1)$'s, as shown in Fig. 4(*b*). Not only the interrelation of the three largest strains, but their independence of the detailed symmetry of the felspar, and their dependence on cation valency, are thus explained simultaneously. (It may be noted in passing that since $O_A(2)$ is abnormally close to Ca it is in a strong electrostatic field and is polarized accordingly, with consequent effect on its other bonds).

4. Linkages and stability of structure

4·1. *Monoclinic approximation*

We now consider the linked framework as a whole, to see how the details hitherto examined fall into place. Figs. 5(*a*), (*b*), (*c*), are stylized diagrams of parts of the structure; (*a*) and (*b*) are viewed down [010], and may be compared with the scale diagram in Fig. 1,

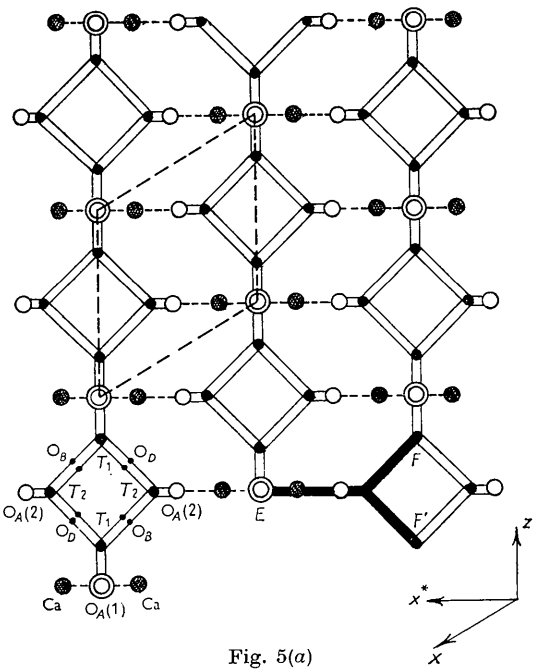

Fig. 5(*a*)

Fig. 5. Stylized diagrams of parts of structure. (*a*) Projection on (010) of slab bounded approximately by $y = \pm 0{\cdot}3$, (*b*) projection on (010) of slab bounded approximately by $y = 0{\cdot}1$, $0{\cdot}4$, (*c*) projection down [001] of whole 7 Å cell. In (*a*) and (*b*) the 7 Å cell is outlined by dashed lines. Pairs of atoms and bonds which are superposed in projection are shown by double lines. Heavy lines E–(F, F') and G–H indicate links affecting x^* repeat distance. Labelling of atoms is given in bottom left-hand corner.

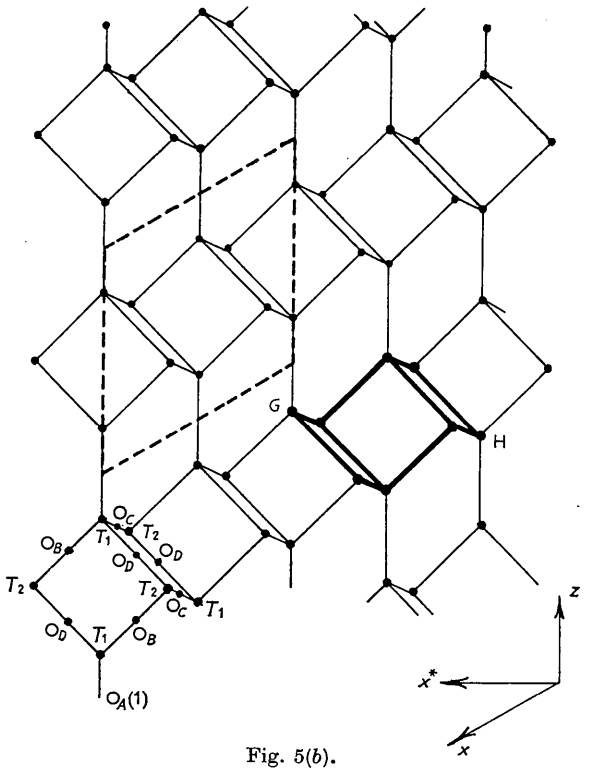

Fig. 5(*b*).

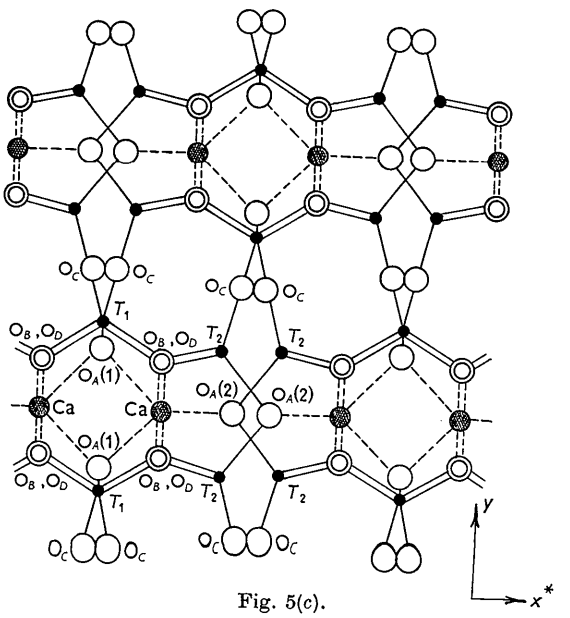

Fig. 5(*c*).

and (*c*) is viewed down [001]. Neither in Fig. 5 nor in the following discussion is any distinction made between Si and Al, because, as has been shown above, their difference gives only second-order effects. The full sanidine symmetry is retained for this first stage of the discussion.

Fig. 5(*a*), which includes all atoms except O_C, shows the striking pseudosymmetry which exists within a (010) slab of the structure bounded approximately by $y = \pm 0{\cdot}2$. To this approximation, atoms O_B and O_D are equivalent, and the symmetry is orthorhombic, atoms Ca, $O_A(1)$ and $O_A(2)$ each lying at the intersection of two mirror planes. The slab is built from a double sheet of *T*–O tetrahedra, each sheet containing four-membered rings bound tightly to rings in the other sheet by a complex system of cross-girders emanating from Ca and $O_A(2)$ (Fig. 5(*c*)). Obviously the whole slab forms a fairly rigid unit.

Fig. 5(*b*) shows the linkage between one slab and the next, between the upper rings of the slab in 5(*a*) (centred on $y=0$) and the lower rings of the one above it (centred on $y=\frac{1}{2}$). The linkage is through O_C. The orthorhombic pseudosymmetry has completely disappeared. Atoms O_D are topologically distinguished from O_B by their participation in a four-membered ring with O_C, which stands in a vertical plane linking the layers.

The repeat distance in the x^* direction is determined by two different sets of links, shown in Figs. 5(*a*) and (*b*) by the heavily-drawn lines *E*–(*F*, *F*′) and *G*–*H* respectively. Other links are negligible, tending mainly to produce shear. For equilibrium, the stresses in *E*–(*F*, *F*′) and *G*–*H* must be equal and opposite.

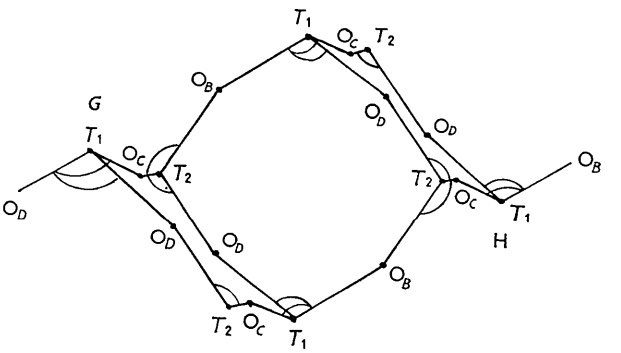

Fig. 6. Stylized diagram showing detail of linkage in region *G*–*H* of Fig. 5(*b*).

But we have seen that *E*–(*F*, *F*′) is in compression, shown by the shortness of the bond Ca–$O_A(2)$. Hence *G*–*H* must be in tension. This is shown in more detail in Fig. 6 (cf. also 5(*c*)). Assuming that the stress manifests itself more in bond angle strains than in *T*–O bond length strains, we expect positive strains in the angles marked in Fig. 6, and negative strains in $T_2(BD)$ and $T_2(AC)$, the latter rotating the bond T_2–O_C downwards towards the plane of the paper. The angle $T_1(BD)$ is also concerned in the link *E*–(*F*, *F*′), where a negative strain is required, but its effect on this length is only half its effect on *G*–*H*, and may therefore be ignored; on the other hand, $T_2(BD)$ should have a positive strain in *E*–(*F*, *F*′) and we cannot predict whether this or the negative strain required for *G*–*H* will predominate. Table 12 shows a comparison of predicted and observed strains

Table 12. *Comparison of observed and predicted bond angle strain in x* repeat distance*

	Mean bond-angle strain (degrees)					
	$T_1(BC)$	$T_1(BD)$	$T_2(AC)$	$T_2(BC)$	$T_2(BD)$	$T_2(CD)$
Predicted	+	+	−	+	Indeterminate	+
Anorthite	+2·6	+4·4	−6·1	+2·4	+0·6	+4·9
Celsian	+3·0	+4·2	−7·3	+3·0	+2·9	+3·6
Low albite	−0·6	+1·2	−5·0	+3·5	+1·0	+2·1
High albite	−1·5	+3·0	−2·5	−1·8	+1·3	+7·4
Microcline	+3·2	+0·2	−4·3	+1·2	+1·2	+3·3
Orthoclase	+0·7	+0·5	−4·9	+1·8	+1·6	+1·3
Sanidine	+1·4	+2·4	−4·9	+0·4	+2·1	+2·3

for these angles in all felspars. The agreement is very good for anorthite and celsian, and the same trend can be seen in the other felspars, though with more irregularities. Possibly this good agreement, and the regular distribution of strain it entails, are associated with the stability of the anorthite structure.

Fig. 5(*c*) shows part of the structure viewed down [001]. The complexity of the linkages in the double layers near $y=0$ and $\frac{1}{2}$ is very evident, and contrasts with their paucity between double layers. One would expect to find the structure amenable to shear in this plane. The observed lack of strain in the O_C angles (Table 2(*g*)) suggests that they can adjust themselves independently of internal changes in the double layers, at the cost of lateral displacement, resulting macroscopically in changes of α and γ angles.

4·2. *Distortion from monoclinic symmetry*

The next step is to examine what distortions follow as a result of the small Ca radius.

In Fig. 3(*a*) it was shown that the x^* coordinate of Ca is rather rigidly determined. In the (001) plane, however, the approximation of Fig. 5(*a*) shows that Ca has four equidistant O_B and O_D neighbours, which cannot all come into contact with it because they are impeded by $O_A(1)$ and $O_A(2)$. For the larger cations K and Ba, they can do so, and the cation remains on, or very close to, the symmetry plane. But the smaller Ca moves off the symmetry plane along one diagonal of the square $O_BO_DO_DO_B$, and these O's readjust themselves so that three make good contact and one is pushed right out, its bond angle increasing to about 170° in the process.

These displacements of O cause stresses in the framework which cannot be entirely accommodated by strains in the nearest T–O bonds and T bond angles. The tetrahedra are rotated or displaced, and so transmit part of the strain to their neighbours. If the next Ca atom is fairly close, its direction of displacement may be determined by that of the first. In this way the displacements may be cooperative either over closed groups of atoms or over the whole periodic structure.

The detailed pattern of Ca displacement in anorthite can be predicted qualitatively with the help of two general principles: (i) that when strong internal

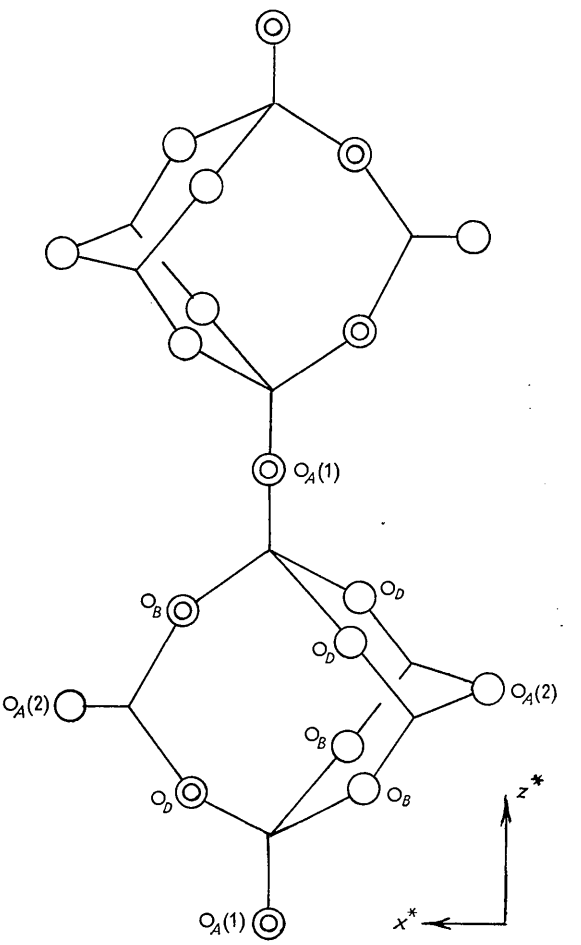

Fig. 7. Schematic projection of double layer on (010), showing distortion from original symmetry due to small Ca.

stresses are related by symmetry or pseudosymmetry in the ideal structure, this symmetry will be retained, at least locally, in the distorted structure, (ii) that all periodicities will remain as small as is compatible with (i). In anorthite, there are strong oppositely-directed electrostatic repulsions acting along Ca–Ca across the centre of symmetry at (0, 0, 0); this centre is retained. There is a strong compression along Ca–$O_A(2)$; this direction remains, locally, an axis

of pseudosymmetry, and the plane defined by T_2–$O_A(2)$–T_2 tilts about it, out of the vertical, giving equal rotations (or displacements) to the two T_2 octahedra and their adjacent O's (Fig. 7). In this way large bond-angle strains can be introduced at O_B and O_D, without change of bond length. Since there is one large O-angle for every Ca, and two are associated with every $O_A(2)$, half the $O_A(2)$'s are unaffected. Those affected are (like everything else) centrosymmetric about (0, 0, 0) (Fig. 7). Hence successive double rings in the z direction cannot be true repeats; exact repetition occurs only after twice the original c distance. There is nothing in the sideways linkage to forbid the original C-face-centred arrangement, which is therefore retained. A body-centred arrangement would have the disadvantage, because of its centre of symmetry at $(\frac{1}{4}, \frac{1}{4}, \frac{1}{2})$ (referred to the cell in Fig. 5(a) and (b)), of introducing two 170° angles into the same vertical 4-membered ring, which looks unlikely.

The features illustrated schematically in Fig. 7 can be seen in the projection of the actual structure, Fig. 1 (best shown in 1(a)).

The argument thus predicts a 14 Å C-face-centred structure, having the environments of Ca(000) and Ca(zi0) identical with each other and different from those of Ca(z00) and Ca(0i0). This result, as was made clear in Paper I, is a very good approximation to observed fact. The Si/Al alternation, however, does not satisfy the C-face-centring condition, and the consequent atomic displacements result in small differences between members of each of the above pairs.

The argument would apply equally to albite, except that the electrostatic forces and their resultant strains are smaller, and mistakes of sequence therefore more likely. This point will be discussed elsewhere.

No use has been made here of the individual bond-angle strains at T which show departures from monoclinic symmetry. These, and the individual bond angles at O, may contain much useful information. The structure also offers opportunities for studying lattice parameters in terms of interatomic forces, along the lines suggested in § 4·1. On both these points, it would be particularly valuable to trace the changes of structural detail which accompany macroscopic changes and changes of composition. Structure determinations of other felspars in the plagioclase series are in progress (Chandrasekhar, Fleet & Megaw, 1960; Kempster, 1957; Waring, 1961), and further discussions may wait till anorthite can be compared with them.

5. Summary

The unit cell of anorthite consists of four subcells of equal volume in which the atoms have nearly but not quite identical configurations. The structure is perfect, with no disorder, within the limits of accuracy of the work, which are fairly narrow. Si and Al tetrahedra alternate so that every oxygen has one Si neighbour and one Al. This distribution means that pairs of subcells related by the body-centring vector have the same Si/Al distribution; nevertheless their atomic coordinates are not as closely similar as pairs which have unlike distribution, and are related by C-face-centring. The tetrahedra are not perfectly regular—an effect observed in earlier felspar studies concerning bond angles, and here extended to their bond lengths. Small differences in tetrahedral mean bond lengths are rather less than would have been expected from the scatter of lengths within tetrahedra, but greater than is allowed for in Smith's original discussion of bond lengths.

One Ca atom is perhaps best considered as 6-coordinated, though with a 7th more distant neighbour; the other three are 7-coordinated. All the Ca bond lengths are fairly normal; the closest contact is to $O_A(2)$, which is a short bond in other felspars. Though the Ca environments (the 'cavities' in the structure) are of different shapes, there is no evidence that any of them has a possible alternative site giving reasonable bond lengths to the oxygens surrounding.

The temperature factors, though not determined with great accuracy, are informative. The low values of B for Si/Al and O are characteristic of a perfect structure (as contrasted with the B value for oxygen in felspars with Si/Al disorder, which includes a 'broadening factor'). The high value for Ca is comparable with that in other felspars, and may represent either a true or a frozen-in thermal amplitude.

The 'strains' (departures from ideal values) of bond length and bond angle give important information. Individual Si–O and Al–O bonds show, on the average, significant decreases as the number of Ca neighbours of the O drops from 2 to zero. The bond angle strains at all T atoms of the same crystallographic type (T_1 or T_2) show marked similarity, independent of symmetry or Si/Al ratio in different felspars; the three largest, in particular, can be shown to depend on cation charge rather than cation size. The role played by cation–cation repulsion across the symmetry centre (0, 0, 0) is very important. It controls not only the distortions of the tetrahedra compatible with monoclinic symmetry, but also the pattern of displacements and rotations consequent on the relatively small size of Ca. Consideration of its effect on the x^* repeat distance leads to a qualitative prediction of bond-angle strain in the other Si and Al angles which agrees with that observed. Consideration of its effect on Ca displacement predicts the close approximation to a C-face-centred lattice which is also found experimentally.

It is rather surprising that the explanation of the structure can be carried so far without any need to invoke the effects of differences between Si and Al in either radius or charge. Obviously these must play a part; but it would appear that the part is smaller than has often been tacitly assumed. Deviations of

individual values of bond lengths and bond angles from their group averages give a basis for further study.

It is a pleasure to express our indebtedness to Dr W. H. Taylor for suggesting this work, and for his support and guidance throughout its execution. It will be obvious how much it owes to his forethought and wise planning, by which detailed structural studies of the key members of the felspar family have been made available for comparison with each other. We are grateful to Mr P. H. Ribbe for carrying out the bond angle calculations.

References

BAKAKIN, V. V. & BELOV, N. V. (1960). *Kristallografiya*, **5**, 864.
BAILEY, S. W. & TAYLOR, W. H. (1955). *Acta Cryst.* **8**, 621.
CHANDRASEKHAR, S., FLEET, S. G. & MEGAW, H. D. (1960). *Abstract, Congress of International Mineralogical Association*, Copenhagen, 1960.
CLARK, J. R. & APPLEMAN, D. E. (1960). *Science*, **132**, 1837.
COLE, W. F., SØRUM, H. & KENNARD, O. (1949). *Acta Cryst.* **2**, 280.
CRUICKSHANK, D. W. J. (1949). *Acta Cryst.* **2**, 65.
FERGUSON, R. B., TRAILL, R. J. & TAYLOR, W. H. (1958). *Acta Cryst.* **11**, 331.
GOLDSMITH, J. R. & LAVES, F. (1955). *Z. Kristallogr.* **106**, 3.
JONES, J. B. & TAYLOR, W. H. (1961). *Acta Cryst.* **14**, 443.
KEMPSTER, C. J. E. (1957). Thesis, Cambridge University.
KEMPSTER, C. J. E., MEGAW, H. D. & RADOSLOVICH, E. W. (1960). *Acta Cryst.* **13**, 1003.
KEMPSTER, C. J. E., MEGAW, H. D. & RADOSLOVICH, E. W. (1962). *Acta Cryst.* **15**, 1005.
LIEBAU, F. (1960). *Silikattechnik*, **11**, 397.
LOEWENSTEIN, W. (1954). *Amer. Min.* **39**, 92.
MEGAW, H. D. (1956). *Acta Cryst.* **9**, 56.
NEWNHAM, R. E. & MEGAW, H. D. (1960). *Acta Cryst.* **13**, 303.
RADOSLOVICH, E. W. (1960). *Acta Cryst.* **13**, 919.
SMITH, J. V. (1954). *Acta Cryst.* **7**, 479.
SMITH, J. V. (1960). *Acta Cryst.* **13**, 1004.
SMITH, J. V., KARLE, I. L., HAUPTMAN, H. & KARLE, J. (1960). *Acta Cryst.* **13**, 454.
WARING, J. (1961). Thesis, Cambridge University.

Acta Cryst. (1962). **15**, 1035

The Molecular and Crystal Structure of 3-Benzoylanthranil (2-Phenylisoisatogen)

BY M. SUNDARALINGAM AND G. A. JEFFREY

The Crystallography Laboratory, The University of Pittsburgh, Pittsburgh 13, *Pa., U.S.A.*

(*Received* 28 *December* 1961)

The crystal structure investigation of a compound ($C_{14}H_9NO_2$), previously known as 2-phenylisoisatogen, has established its chemical constitution to be that of 3-benzoylanthranil, (or 3 benzoyl 2,1-benzisoxazole). The structure was solved by means of a well-resolved projection down a short axis and was refined with three-dimensional data using differential syntheses and least squares methods. The hydrogen atoms were located by difference syntheses. The configuration of the molecule and the bond lengths are discussed in terms of valence-bond resonance theory.

Introduction

Ruggli (1919) and Ruggli, Caspar & Hegedus (1939) assigned the tricyclic oxide bridge structure, I, to 2-phenylisoisatogen, the isomer obtained by treating 2-phenylisatogen (Baeyer, 1882) with hot methanolic H_2SO_4. A re-examination of this structure by Cohen & Pinkus (1959) cast doubt on the validity of the Ruggli formulation. The more plausible structure, II, was proposed, for which a planar or nearly planar molecule might be resonance stabilized *cis* or *trans* with respect to the central C_7–C_8 bond. This X-ray investigation was initially undertaken to verify this formulation and to decide between the two possible stereo-isomers, II or III. It became possible at an early stage in the analysis to identify the molecule as II, which is 3-benzoylanthranil and this was briefly reported by Pinkus, Cohen, Sundaralingam & Jeffrey (1960). A more detailed study was then pursued because of the interest in the detailed stereochemistry of the molecule and its interpretation in terms of resonance theory.